

# Generate To Adapt: Aligning Domains using Generative Adversarial Networks

Swami Sankaranarayanan \*    Yogesh Balaji \*    Carlos D. Castillo  
 Rama Chellappa  
 UMIACS, University of Maryland, College Park

## Abstract

Visual Domain adaptation is an actively researched problem in Computer Vision. In this work, we propose an approach that leverages unsupervised data to bring the source and target distributions closer in a learned joint feature space. We accomplish this by inducing a symbiotic relationship between the learned embedding and a generative adversarial framework. This is in contrast to methods which use an adversarial framework for realistic data generation and retraining deep models with such data. We show the strength and generality of our method by performing experiments on three different tasks: (1) Digit classification (MNIST, SVHN and USPS datasets) (2) Object recognition using OFFICE dataset and (3) Face recognition using the Celebrity Frontal Profile (CFP) dataset.

## 1. Introduction

The development of powerful learning algorithms such as Convolutional Neural Networks (CNNs) have provided a classic pipeline for solving many classification problems [28]. The abundance of labeled data has resulted in remarkable improvements for tasks such as the Imagenet challenge: beginning with the CNN framework of Krizhevsky *et al* [13] and more recently Resnet [9] and its variants. Another example is the steady improvements in performance on the LFW dataset [26]. The common theme across all these approaches is the dependence on lot of labeled data. While labeled data is available and getting labeled data has been easier over the years, the lack of uniformity of label distributions across different domains results in suboptimal performance of even the powerful CNN-based algorithms on realistic unseen test data. This is abundantly clear in the example of faces where most available labeled data tends to be frontal. Hence the learning algorithm, in general, does not perform equally well across viewpoints. The use of unlabeled target data to mitigate the shift between source and target distributions is the most promising direction domain

\*First two authors contributed equally

adaptation. Hence this paper focuses on the topic of unsupervised domain adaptation.

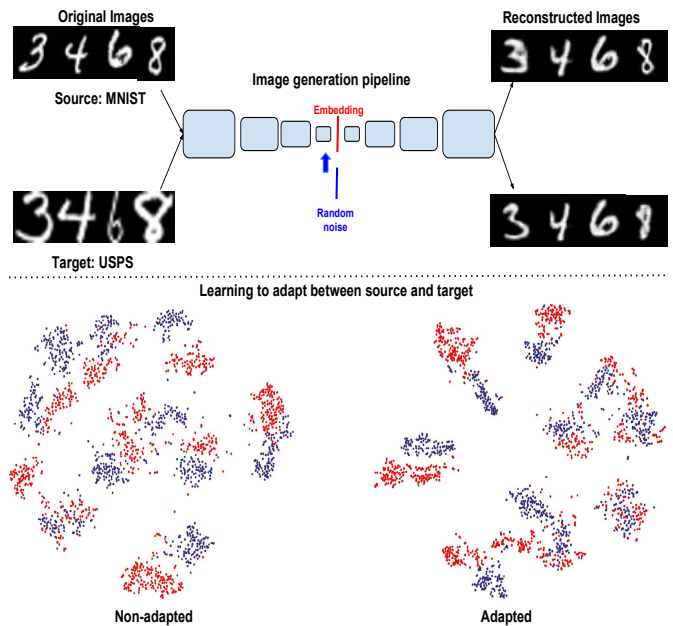


Figure 1. The top half provided an illustration of our image generation pipeline and a visual demonstration of how the proposed approach is able to reconstruct source and target images. The target labels were not used during training. In the bottom half, we show a t-SNE visualization of the unadapted and adapted encoder representations demonstrating how our approach is able to adapt the source and target distributions. Blue dots represent source data and Red dots represent the target data.

In this work, we propose a way to learn an embedding that is robust to the shift between source and target distributions. We intend to achieve this by using unsupervised data sampled from the target distribution to guide the supervised learning procedure that uses data sampled from the source distribution. The main contribution of this work is that we propose an adversarial image generation framework to directly learn the shared feature embedding using labeled data from source and unlabeled data from the target. It should be noted that while several methods have

used an adversarial framework for solving the domain adaptation problem, the novelty of the proposed approach is in using a joint generative discriminative method where the generation is performed using a variant of Generative Adversarial Network (GAN) [7]. During training, the source images are passed through the encoder to obtain an embedding which is then used by the classifier for predicting the source label and also used by the generator to generate a realistic source image. The realistic nature of the images from the generator is controlled by the discriminator. The embedding is updated based on the discriminative gradients from the classifier and generative gradients from the adversarial framework. Given unlabeled target images, the embedding is updated using only gradients from the adversarial part, since the labels are unavailable. Thus, the embedding learns to discriminate better even in the target domain using the knowledge imparted by the generator-discriminator pair. We would like to point out that although the proposed approach uses an image generation procedure for learning the domain shift, the quality of the image reconstruction is not our focus. By using the discriminator as a multi-class classifier, we ensure that the gradient signals backpropagated by the discriminator for the unlabeled target images belong to the feature space of the respective classes. By sampling from the distribution of the generator after training, we show that the network has indeed learnt to bring the source and target distributions closer. The bottom half of figure 1 shows a t-SNE [19] visualization of the embeddings for the MNIST→USPS setting for two cases: (1) Non-adapted: Encoder trained with images from source only (2) Adapted: Encoder trained with the proposed approach. It can be observed that the proposed approach results in a closer match between the source and target distributions. We show examples of such reconstructions in Section 4. To summarize, the major contribution of this work is to provide an adversarial image generation framework for unsupervised domain adaptation that directly learns a joint feature space in which the distance between source and target distributions is minimized. Our experiments show that the proposed framework yields superior results compared to similar approaches which update the embedding based on auto-encoders [4] or disentangling the domain information from the embedding by learning a separate domain classifier [3]. This paper is organized as follows: Section 2 describes contemporary approaches for the unsupervised domain adaptation problem and places our work among them. In section 3, we describe in detail the formulation of our approach and the iterative training procedure. In section 4, we describe the experimental setups and discuss the results using both quantitative and qualitative experiments. We conclude this paper in section 5.

## 2. Related Work

Domain adaptation is an actively researched topic in many areas including Machine Learning, Natural Language Processing and Computer Vision. In this section, we focus on visual domain adaptation since it is more relevant to our work. Earlier approaches to domain adaptation focussed on building feature representations that are invariant across domains. This was accomplished either by feature reweighting and selection mechanisms [10] [2], or by learning an explicit feature transformation that aligns source distribution to the target [8] [22] [6].

Recently, Deep Neural Networks have been shown to be successful in learning complex feature representations that enable them to achieve state-of-the-art performance in most machine learning tasks [13] [9]. This ability to learn powerful representations has been harnessed to perform unsupervised domain adaptation in [3][31][16] [18][30]. The underlying idea behind such methods is to minimize a suitable loss function that captures domain discrepancy, in addition to the task being solved.

Deep learning methods for visual domain adaptation can be broadly grouped into few major categories. One line of work uses Maximum Mean Discrepancy (MMD) as a metric to measure the shift across domains. Deep Domain Confusion (DDC) [31] jointly minimizes the classification loss and MMD loss of the last fully connected layer. Deep Adaptation Networks (DAN) [16] extends this idea by embedding all task specific layers in a reproducing kernel Hilbert space and minimizing the MMD in the projected space. In addition to MMD, Residual Transfer Networks (RTN) [18] uses a gated residual layer for classifier adaptation.

Another class of methods uses adversarial losses to perform domain adaptation. Revgrad [3] poses the domain adaptation problem as a minimax game between a domain classifier and a feature extractor. The goal of the feature extractor is to produce embeddings that fool the domain classifier, while at the same time minimize the classification loss. Adversarial Discriminative Domain Adaptation (ADDA) [30] on the other hand learns separate feature extraction networks for source and target domains, the target CNN is trained so that a domain classifier cannot distinguish the embeddings produced by the source or target CNN.

Adversarial networks have been successfully applied for image generation tasks where the generator network  $G$  and the discriminator network  $D$  compete in a 2-player game [7].  $G$  models the data distribution while  $D$  distinguishes the distribution produced by  $G$  from the true data distribution. Following the success of GAN, several methods have tried to use GAN based approaches for unsupervised domain adaptation. Taigman *et al.* [29] train a cross-domain generative model that maps samples from the source domain to the target domain without utilizing any source-target correspondence. Domain adaptation is then

performed by learning a classifier on the transferred images. Coupled GAN (CoGAN) [15] on the other hand trains a coupled generative model that learns the joint data distribution across the two domains. A domain invariant classifier is learnt by sharing weights with the discriminator of the CoGAN network.

Unlike the methods discussed above, we use image generation as a sub-task for domain adaptation. Related works that use a similar approach are Deep Reconstruction Classification Networks(DRCN) [4] and Domain Separation Networks(DSN) [1]. DRCN uses feature embedding to multitask source label prediction and target image reconstruction. DSN explicitly models the private and shared components of source and target feature representations, and learns such representations using a combination of feature similarity loss and image reconstruction loss. Unlike these methods, we enforce the domain alignment constraint strongly by training a generative model for the source data, and forcing the encoder to produce the embeddings for the target data, which when fed to the generative model produces good source-like images.

### 3. Method

In this section, we provide a formal treatment of the proposed approach and explain in detail our iterative optimization procedure. Let  $\mathbf{X} = \{x_i\}_{i=1}^N$  be an input space of images and  $\mathbf{Y} = \{y_i\}_{i=1}^N$  be the label space. We assume there exists a source distribution,  $\mathcal{S}(x, y)$  and target distribution  $\mathcal{T}(x, y)$  over the samples in  $\mathbf{X}$ . In unsupervised domain adaptation, we have access to the source distribution using labeled data from  $\mathbf{X}$  and the target distribution via unlabeled data sampled from  $\mathbf{X}$ . Operationally, the problem of unsupervised domain adaptation can be stated as learning a predictor that is optimal in the joint distribution space  $\mathcal{S} \otimes \mathcal{T}$  by using labeled source data and unlabeled target data sampled from  $\mathbf{X}$ . We consider problems where the data from  $\mathbf{X}$  have discrete labels from the set  $\mathbf{L} = \{1, 2, 3, \dots, N_c\}$ , where  $N_c$  is the total number of classes. Our objective is to learn an embedding map  $F : \mathbf{X} \mapsto \mathbb{R}^d$  that is used by a prediction function  $C : \mathbb{R}^d \mapsto \mathbf{L}$ . The predictor has access only to the labels for the data sampled from the source distribution and not from the target distribution. By extracting information from the target data during training,  $F$  implicitly learns the domain shift between  $\mathcal{S}$  and  $\mathcal{T}$ . In the rest of this section, we use the terms source (target) distribution and source (target) domain interchangeably.

As explained in section 2, several approaches including learning entropy-based metrics, learning a domain classifier based on a embedding network or denoising autoencoders have been used to transfer information between the source and target distributions. In this work, we use a GAN to help the embedding bridge the gap between source and target domains, since this enables a rich information transfer by

using both a generative and a discriminative process. In a traditional GAN, two competing mappings are learned: the discriminator  $D$  and the generator  $G$ , both of which are modeled as deep neural networks.  $G$  and  $D$  play a minimax game where  $D$  tries to classify the generated samples as fake and  $G$  tries to fool  $D$  by producing examples that are as realistic as possible. More formally, to train a GAN, the following optimization problem is solved in an alternative manner:

$$\min_G \max_D \mathbf{E}_{x \sim p_{data}} (\log(D(x))) + \mathbf{E}_{z \sim p_{noise}} \log(1 - D \circ G(z)) \quad (1)$$

As an extension to traditional GANs, conditional GANs [20] enable conditioning the generator and discriminator mappings on additional data such as a class label or an embedding. They have been shown to generate images of digits and faces conditioned on the class label or the embedding respectively [29]. Training a conditional GAN involves optimizing the following minimax objective:

$$\min_G \max_D \mathbf{E}_{x \sim p_{data}} (\log(D(x))) + \mathbf{E}_{\{z \sim p_{noise}, y\}} \log(1 - D \circ G(y, z)) \quad (2)$$

In this work, we employ a conditional GAN by conditioning the generator using the embedding. Specifically, the input to the generator is a concatenated version of the embedding and a random noise vector :  $[F(x), z]$  where  $z \in \mathcal{N}(0, 1)$ ;  $F$  is the encoder mapping and  $[...]$  represents vector concatenation. The dimensionality of  $z$  is a hyperparameter of our method; however for all our experiments we have achieved consistent performance by setting it equal to the dimensionality of  $F$ . The intuition behind using a random noise vector is to give the generator some extra degrees of freedom to model external variations that are absent in the source data. The discriminator mapping  $D$  is a  $(N_c+1)$ -way classifier taking labels from the set  $\mathbf{L}_D = \{\mathbf{L} \cup \{N_c + 1\}\}$ , with  $N_c$  real classes and an extra class being the fake class. We denote the set  $\{1, 2, \dots, N_c\}$  as real labels and  $N_c + 1$  as the fake label. The inputs to  $D$  can be real images from the source domain or generated fake images from the source or target domains. To jointly learn the embedding and the generator-discriminator pair, we employ an alternating optimization procedure:

1. Given labeled source images as input,  $D$  classifies the real images into one of the real classes and classifies the generated fake images into the fake class.
2. Using the gradients from  $D$ ,  $G$  is updated to produce realistic class consistent source images.
3.  $F$  and  $C$  are updated based on the source images and real labels in a traditional supervised manner.

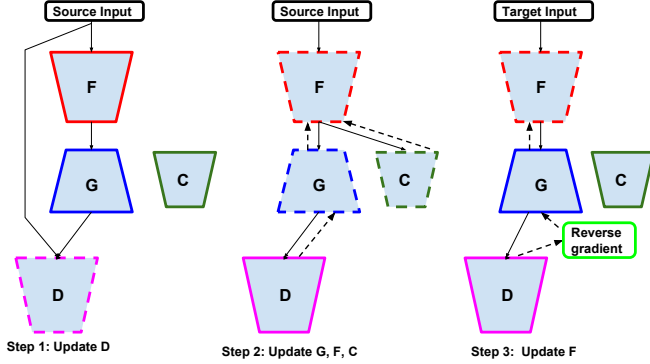


Figure 2. The data flow during forward pass (solid lines) and gradients during backward pass (dashed lines) are shown. A dashed boundary for a block implies that block is being updated and solid boundary implies it is held fixed.

4. In the final step, given the target images, we update  $F$  by minimizing the probability of  $D$  to classify the generated target images as fake.

For ease of implementation, steps 2 and 3 are combined into a single update. Figure 2 shows the direction of data and gradient flow through our setup in each optimization step.

**Use of target data:** The main strength of our approach is how the target images are used to update the embedding. Given a batch of target images  $[x_i]_{i=1}^N$  as input, we update the embedding  $F$  by *reversing* the gradients of the following loss function:

$$\sum_{i=1}^N \log(1 - D \circ G([F(x_i), z_i])) \quad (3)$$

where  $z_i$  a random noise vector sampled from  $\mathcal{N}(0, 1)$ . The loss in (3) encourages  $D$  to classify the target images as fake. Our objective during the target update step is that: For the target domain, the embedding should be learnt so that  $G$ , conditioned on the embedding, produces source-like images that fool  $D$ . If this is achieved optimally, then one can infer that the embedding has fully learnt to map the target distribution to the source distribution. To enable this behavior, the loss function in (3) is used to update the embedding by *reversing* the gradient of the discriminator corresponding to the fake label. This update will enable  $F$  to preserve the class information for the target domain due to the following reason: During the source update step, both  $F$  and  $D$  are learned in a class consistent manner using labels from the source domain. As training progresses, the reversed gradients that are used to update the embedding become well conditioned on the actual class of the target image even though target label information is never provided. This symbiotic relationship between the embedding

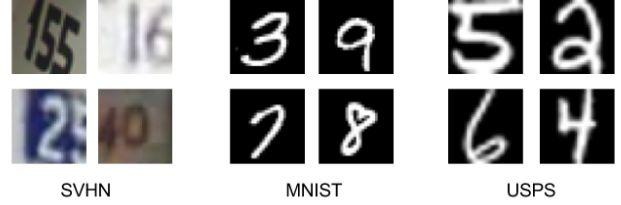


Figure 3. Visualization of digit datasets

and the adversarial framework contributes to the success of the proposed approach. It should be noted that the gradient signals from (3) are used to update  $F$  only and reversal of the gradient is performed as shown in figure 2.

Our iterative optimization procedure can be summarized as follows:

- For source images, we update the mappings  $D$ ,  $G$ ,  $C$  and  $F$  using the gradient of the loss function:

$$\begin{aligned} L_{src} &= \lambda L_{adv} + L_{cls} \text{ where,} \\ L_{adv} &= \min_F \min_G \max_D \mathbf{E}_{x \sim \mathcal{S}} \log(D(x) + \\ &\quad \mathbf{E}_{\{z \sim p_{noise}, x \sim \mathcal{S}\}} \log(1 - D \circ G([F(x), z])) \\ L_{cls} &= \min_F \min_C \mathbf{E}_{x \sim \mathcal{S}} \log(C \circ F(x)) \end{aligned} \quad (8)$$

$\lambda$  is the coefficient that trades off between the classification loss and the adversarial loss.

- For the target images, the loss function involves updating only the embedding  $F$  and does not involve the classifier, since no target labels are observed during training.

$$L_{tgt} = \max_F \mathbf{E}_{x \sim \mathcal{T}, z \sim p_{noise}} - \log(1 - D \circ G([F(x), z])) \quad (9)$$

The pseudocode for this iterative procedure is given in Algorithm 1. We find that our approach is not overly sensitive to the cost coefficient  $\lambda$ . However, the value of the parameter is dependent on the application and size of the dataset. Such specifications are mentioned in section 4.

## 4. Experiments and Results

This section reports the experimental validation of our method. To demonstrate the versatility of our approach, we perform experiments on three different tasks that span across multiple domains - digit recognition, object recognition and face recognition. In the process, we also test the sensitivity of our approach to the size of dataset. Each dataset we experimented on, varies greatly in size, with some containing just a few hundred images to others having tens of thousands of images.

---

**Algorithm 1** Iterative training procedure of our approach

---

- 1: training iterations = N
- 2: **for** t in 1:N **do**
- 3:   Sample  $k$  images from source domain  $\mathcal{S}$ :  $\{s_i, y_i\}_{i=1}^k$
- 4:   Let  $f_i = F(s_i)$  be the embeddings computed for the source images.
- 5:   Sample  $k$  random noise samples  $\{z_i\}_{i=1}^k \sim \mathcal{N}(0, 1)$ , where  $\dim(z_i) = \dim(F(s_i))$
- 6:   Update discriminator to classify real/fake samples using the adversarial loss.

$$\max_D \frac{1}{k} \sum_{i=1}^k [\log(D(s_i)) + \log(1 - D \circ G([f_i : z_i]))] \quad (4)$$

- 7:   Update the generator through the discriminator gradients computed using real labels.

$$\min_G \frac{1}{k} \sum_{i=1}^k [\log(1 - D \circ G([f_i : z_i]))] \quad (5)$$

- 8:   Update the embedding using a linear combination of the adversarial loss and classification loss.

$$\min_F \frac{1}{k} \sum_{i=1}^k [\log(C(f_i)) + \lambda \log(1 - D \circ G([f_i : z_i]))] \quad (6)$$

- 9:   Sample  $k$  images from target domain  $\mathcal{T}$ :  $\{t_i\}_{i=1}^k$
- 10:   Let  $f_i = F(t_i)$  be the embeddings computed for the target images.
- 11:   Sample  $k$  random noise samples  $\{z_i\}_{i=1}^k \sim \mathcal{N}(0, 1)$ , where  $\dim(z_i) = \dim(F(t_i))$
- 12:   Update the embedding by minimizing the likelihood (or maximizing the negative log likelihood) of the target images being classified as fake by the discriminator.

$$\max_F \frac{1}{k} \sum_{i=1}^k [-\log(1 - D \circ G([f_i : z_i]))] \quad (7)$$

13: **end for**

---

Table 1. Accuracy (mean  $\pm$  std%) values for cross-domain recognition tasks over five independent runs on the digits based datasets. The best numbers are indicated in **bold** and the second best are underlined. - denotes unreported results. MN: MNIST, US: USPS, SV: SVHN

Method	MN $\rightarrow$ US	US $\rightarrow$ MN	SV $\rightarrow$ MN	MN $\rightarrow$ SV
Source only	75.2 $\pm$ 1.6	57.1 $\pm$ 1.7	60.3 $\pm$ 1.5	26.0 $\pm$ 1.2
RevGrad [3]	77.1 $\pm$ 1.8	73.0 $\pm$ 2.0	73.9	-
DRCN* [4]	<u>91.8</u> $\pm$ 0.09	73.7 $\pm$ 0.04	<u>82.0</u> $\pm$ 0.16	<b>40.1</b> $\pm$ 0.07
CoGAN [15]	91.2 $\pm$ 0.8	89.1 $\pm$ 0.8	-	-
ADDA [30]	89.4 $\pm$ 0.2	<u>90.1</u> $\pm$ 0.8	76.0 $\pm$ 1.8	-
Ours	<b>92.5</b> $\pm$ 0.7	<b>90.8</b> $\pm$ 1.3	<b>84.7</b> $\pm$ 0.9	<u>36.4</u> $\pm$ 1.2

\* DRCN approach uses more convolutional filters and cross-validates the number of neurons in fully connected layers

### 4.1. Digit Experiments

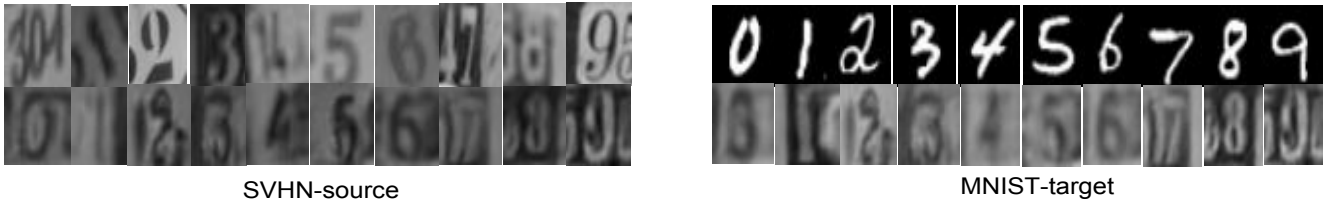
In the first set of experiments, we validate our method by performing domain adaptation on three standard digit datasets - MNIST [14], USPS [11] and SVHN [21]. Each dataset contains digits belonging to 10 classes (0-9), each captured under different conditions. We test the four common domain adaptation settings: SVHN  $\rightarrow$  MNIST,

MNIST  $\rightarrow$  SVHN, MNIST  $\rightarrow$  USPS and USPS  $\rightarrow$  MNIST. In each setting, we use the label information only from the source domain, thus following the unsupervised protocol.

MNIST and USPS are large datasets of handwritten digits captured under constrained conditions. Both these domains are visually very similar and this makes adaptation relatively easy. SVHN dataset, on the other hand was ob-



## SVHN to MNIST



## MNIST to USPS

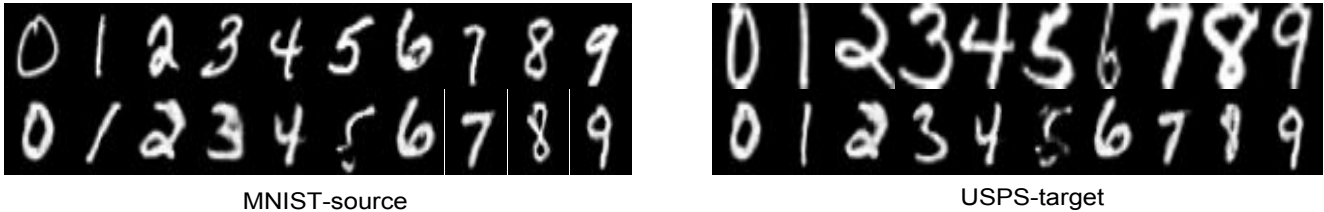


Figure 4. In each set of images, the top row shows the original images and the bottom row shows the reconstructed images from the respective dataset. The top half shows the reconstructions for SVHN  $\rightarrow$  MNIST task and the bottom half for MNIST  $\rightarrow$  USPS task.

tained by cropping house numbers in Google Street View images and hence captures much more diversity. As can be seen from Figure 3, in the SVHN dataset, there is significantly more domain shift with respect to the other two datasets which makes adaptation hard.

**Architecture and Preprocessing** For all digit experiments, following other recent works [3][30], we use a modified version of Lenet architecture as our encoder. The encoder pipeline has three  $5 \times 5$  convolution layers containing 64, 64 and 128 filters respectively, followed by ReLU and pooling. This maps a  $32 \times 32$  image to a 128 dimensional embedding. The label predictor containing two FC layers ( $128 \rightarrow 128 \rightarrow 10$ ) maps this 128 dimensional embedding to a 10 dimensional vector. The generator architecture was adopted from DCGAN [23] - it contains 4 full convolution layers with 512, 256, 128 and 1 filters respectively, each followed by ReLU and batch normalization except the last layer. The output of the last layer is the generated image. The discriminator architecture contains three convolutional layers with 64, 128 and 256 filters, followed by two fully connected layers of size 128 and 11. We used Adam solver [12] with base learning rate of 0.0002 to train our models. The cost coefficient  $\lambda$  is set to 0.1. We resize all input images to  $32 \times 32$  and scale their values to the range  $[0, 1]$ . No data augmentation was performed.

### (a) MNIST $\leftrightarrow$ USPS

We start with the easy case of adaptation involving MNIST and USPS. The MNIST dataset is split into 60000 training and 10000 test images, while the USPS contains 7291 training and 2007 test images. In our experiments, we fol-

low the protocol established in [17], sampling 2000 images from MNIST and 1800 images from USPS. Since random sampling is prone to high variance in performance, we conduct five independent runs, sampling data randomly in each run and report the average performance. We observe that our method performs well in both directions, MNIST  $\rightarrow$  SVHN and SVHN  $\rightarrow$  MNIST. Specifically, we achieve the best performance of 92.5% in MNIST  $\rightarrow$  USPS and 90.8% in USPS  $\rightarrow$  MNIST among the compared methods.

### (b) SVHN $\leftrightarrow$ MNIST

Compared to the previous experiment, SVHN  $\leftrightarrow$  MNIST presents a harder case of domain adaptation owing to larger domain gap. Following other works [3] [30], we use the entire training set (73257 SVHN images and 60000 MNIST images) to train our model, and evaluate on the test set of target domain. Adaptation is much harder in MNIST  $\rightarrow$  SVHN direction compared to SVHN  $\rightarrow$  MNIST, as SVHN is more diverse than the constrained MNIST dataset. In fact, most methods fail to adapt [3], or did not report results in this setting. However, our method achieves 36.4% accuracy, which is 10% higher than the baseline. We would like to point out that the best performing method DRCN uses data augmentation and denoising to improve their performance, none of which we perform. In addition, they use more filters in the convolutional layers and select their model architecture by cross-validating the number of neurons in the fully connected layers. On the other hand, we use a fixed standard architecture for all our experiments. In SVHN  $\rightarrow$  MNIST, our method performs considerably better than other methods achieving state-of-the-art accuracy of 84.7%. A sam-



Figure 5. Visualization of office datasets

ple of reconstructions obtained from our approach for two tasks, SVHN  $\rightarrow$  MNIST and MNIST  $\rightarrow$  USPS are visualized in Figure 4.

## 4.2. OFFICE dataset

The next set of experiments involve the OFFICE dataset, which is a small scale dataset containing images belonging to 31 classes from three domains - Amazon, Webcam and DSLR, each containing 2817, 795 and 498 images respectively. The small dataset size poses a challenge to our approach since we rely on GAN which demands more data for better image generation. Nevertheless, we perform experiments on OFFICE dataset since our interest is not in generating good images, rather in utilizing the generative process to obtain domain invariant feature representations.

**Architecture and Preprocessing** Training deep networks from scratch on small datasets give poor performance. So, an effective technique used in practice is to fine-tune networks trained on a related task having large data [32]. Following other domain adaptation works [3] [4] [18], we use a pre-trained Alexnet model trained on Imagenet as our encoder. We plug in an FC layer to the encoder to produce a 256 dimensional vector output, which we use as our feature embedding. The generator contains 5 full convolution layers with 1024, 512, 256, 128 and 1 filters respectively, each followed by ReLU and batch normalization except the last layer. Each layer upsamples its input to twice the size. The output of the last layer is the generated image. The discriminator architecture contains four convolutional layers with 128, 128 and 128 filters each of size  $5 \times 5$  except the last layer whose filters are  $5 \times 5$ . This is followed by three fully connected layers of size 500, 500 and 32. We initialize all newly added layers using the method of Glorot *et al.* [5] and learn them from scratch. It should be noted that even though the inputs are  $224 \times 224$ , the generator is made to reconstruct a downsampled version of size  $64 \times 64$ . We use Adam solver for optimization with a base learning rate of 0.0002 and momentum 0.8. The dimension of the random noise vector is set to the dimension as the encoder representation, which in this case is 256. The cost coefficient  $\lambda$  is set as 0.1. We first resize all images to  $256 \times 256$  and then randomly select  $224 \times 224$  crops as input images. In addition to random cropping, we also perform random

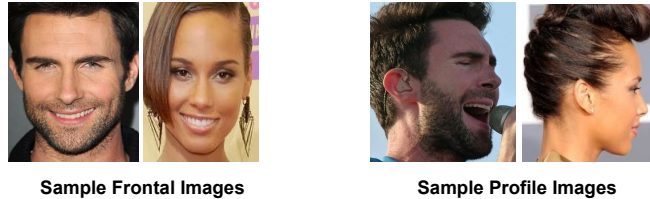


Figure 6. Visualization of CFP dataset

mirroring. We would like to point out that these are the standard augmentation techniques performed in recent domain adaptation works [3][18][31]

In all our experiments, we follow the standard unsupervised protocol - using the entire labeled data in the source domain and unlabeled data in the target domain. Table 2 reports the performance of our method in comparison to other methods. From these results, we can make the following observation - Our method performs the best when we have more data in the source domain. In particular, we observe good performance improvement with Amazon as source: 0.8% and 3.3% in  $A \rightarrow W$  and  $A \rightarrow D$  respectively. Our method performs on par with the best performing method on the other settings too.

## 4.3. CFP dataset

In this experiment, we evaluate our approach on the domain of faces. The Celebrities in Frontal-Profile (CFP) dataset [27] was curated to evaluate the strength of face verification approaches across pose, more specifically, between frontal pose (yaw  $< 10^\circ$ ) and profile poses (yaw  $> 60^\circ$ ). They argue that commonly used CNN-based approaches that perform well on the frontal pose setting perform poorly on profile pose setting. The dataset contains 500 individuals in total with 10 frontal images and 4 profile images per individual. The CFP dataset defines a verification protocol by providing frontal-frontal and frontal-profile pairs with a 1 or 0 label indicating same/different pair. This protocol does not provide access to class labels during the training phase. Since the focus of the current work is improving classification performance for domain adaptation, we create a modified version of the CFP protocol for face recognition similar to the OFFICE protocol: We treat all frontal images as source and all profile images as target. We then train the compared approaches using labeled source images and unlabeled target images and test them on the target images. We do not consider the adaptation in the opposite direction since it is not a realistic situation. We will make the codes and models publicly available.

**Architecture** Training deep networks for face recognition from scratch using a small dataset leads to severe overfitting. Based on our preliminary experiment done by fine-tuning Alexnet [13] on this dataset, we achieved very low Rank-1 accuracy on the target images. Hence, we test

Table 2. Accuracy (mean  $\pm$  std%) values on the OFFICE dataset for the standard protocol for unsupervised domain adaptation [6]. Results are reported as an average over 5 independent runs. The best numbers are indicated in **bold** and the second best are underlined. – denotes unreported results. A: Amazon, W: Webcam, D: DSLR

Method	A $\rightarrow$ W	W $\rightarrow$ A	A $\rightarrow$ D	D $\rightarrow$ A	W $\rightarrow$ D	D $\rightarrow$ W	Average
Alexnet - Source only	61.1 $\pm$ 0.5	48.6 $\pm$ 0.4	64.4 $\pm$ 0.3	46.1 $\pm$ 0.6	99.1 $\pm$ 0.2	95.6 $\pm$ 0.3	69.1
DDC [31]	61.0 $\pm$ 0.5	49.4 $\pm$ 0.6	64.9 $\pm$ 0.4	47.2 $\pm$ 0.5	98.5 $\pm$ 0.3	95.0 $\pm$ 0.3	69.3
DAN [16]	68.5 $\pm$ 0.3	49.8 $\pm$ 0.3	66.8 $\pm$ 0.2	50.0 $\pm$ 0.4	99.0 $\pm$ 0.1	96.0 $\pm$ 0.1	71.7
RevGrad [3]	73.0 $\pm$ 0.6	-	-	-	99.2 $\pm$ 0.3	96.4 $\pm$ 0.4	-
RTN [18]	<u>73.3</u> $\pm$ 0.3	51.1 $\pm$ 0.5	<u>71.0</u> $\pm$ 0.2	50.5 $\pm$ 0.3	<b>99.6</b> $\pm$ 0.1	<b>96.8</b> $\pm$ 0.2	<u>73.7</u>
DRCN [4]	68.7 $\pm$ 0.3	<b>54.9</b> $\pm$ 0.5	66.8 $\pm$ 0.5	<b>56.0</b> $\pm$ 0.5	99.0 $\pm$ 0.2	96.4 $\pm$ 0.3	73.6
Ours	<b>74.1</b> $\pm$ 0.5	<u>53.5</u> $\pm$ 0.8	<b>74.3</b> $\pm$ 0.6	<u>50.6</u> $\pm$ 0.7	<u>99.3</u> $\pm$ 0.3	<u>96.6</u> $\pm$ 0.2	<b>74.7</b>

the domain adaptation approaches by initializing our encoder with the weights of a pretrained face recognition network [25]. We add a fully connected layer with 256 neurons which is used as our feature embedding. The same architectures as the OFFICE experiment are used for the classifier and discriminator networks. We find that the generator is unable to reconstruct the full input image of size 224x224, hence it is made to reconstruct only a 32x32 downsampled version of the input. For the generator, we use four full convolution layers. We initialize all newly added layers using the method of Glorot *et al.* [5] and learn them from scratch. We use Adam solver for optimization with a base learning rate of 0.0002 and momentum 0.8. The dimension of the random noise vector is set to the same dimension as the feature embedding. The cost coefficient  $\lambda$  is set as 0.05.

**Preprocessing:** We align all the face images from the CFP dataset using a similarity transformation as required by the pretrained model [25]. The landmarks used for alignment were obtained using the HyperFace approach [24]. The aligned images were then resized to a 256x256 frame. During training, we applied data augmentation in the form of random cropping and mirroring as in the previous experiments. Please note that the same preprocessing and data augmentation techniques were applied to all the approaches compared in Table 3. The inputs to the encoder are subtracted using the mean provided with [25] and hence the discriminator inputs are scaled to be in the range  $[-1, 1]$ .

Method	Rank-1	Rank-5
Source-only	57.8 $\pm$ 0.5	78.1 $\pm$ 0.4
RevGrad [3]	58.5 $\pm$ 0.3	78.7 $\pm$ 0.2
RevGrad++	60.1 $\pm$ 0.4	79.1 $\pm$ 0.3
Ours	<b>62.3</b> $\pm$ 0.5	<b>83.2</b> $\pm$ 0.2

Table 3. Domain adaptation performance on CFP dataset. Rank-1 and Rank-5 accuracies (mean  $\pm$  std%) are reported for all the approaches as an average over 5 independent runs. The CFP dataset has 2000 profile images in total which is used as the target data.

As this is a new dataset for general domain adaptation practitioners, we compare our method with two baselines:

(1) Source only, where we directly fine-tune the encoder and classifier layers in a supervised manner to predict 1 of 500 identities using *only* source data (2) RevGrad, which corresponds to the original architecture from the gradient reversal work [3] (3) RevGrad++, where we make the domain classifier stronger by adding more neurons to the fully connected layers. The original RevGrad approach has a (1024 $\rightarrow$ 1024) architecture for the domain classifier while the stronger architecture we use has a (3072 $\rightarrow$ 2048) architecture. We used this stronger architecture for gradient reversal in order to provide a fair comparison. Except the source only baseline, other methods are trained using labeled source data and unlabeled target data. The results of the CFP experiment is shown in Table 3. The reported numbers are Rank-1 and Rank-5 accuracies of the compared methods. Note that a strong pretrained model used as our baseline network, still yields only with 57.8% Rank-1 accuracy even after finetuning on this dataset using labeled source data. The RevGrad and RevGrad++ approaches yield only moderate improvements over the source only baseline. In comparison, our approach yields a significant improvement ( $\sim$ 4.5%) over the source-only baseline on Rank-1 accuracy and outperforms the stronger RevGrad++ baseline by  $\sim$ 2.2%. We show a significant improvement over the compared methods on Rank-5 accuracy by outperforming the closest method by 4.1%. This shows that our method is able to leverage target data even in a difficult case such as frontal to profile comparisons.

## 5. Conclusion and Future Work

In this paper, we have addressed the problem of unsupervised domain adaptation. We proposed a joint adversarial-discriminative approach that transfers the information of the target distribution to the learned embedding using a generator-discriminator pair. We have shown the superiority of our approach over existing methods that address this problem using experiments on three different tasks, thus making our approach more generally applicable and versatile. Some avenues for future work include using stronger encoder architectures and applications of our approach to more domain adaptation problems such as RGB-D object



recognition and medical imaging.

## Acknowledgement

This research is based upon work supported by the Office of the Director of National Intelligence (ODNI), Intelligence Advanced Research Projects Activity (IARPA), via IARPA R&D Contract No. 2014-14071600012. The views and conclusions contained herein are those of the authors and should not be interpreted as necessarily representing the official policies or endorsements, either expressed or implied, of the ODNI, IARPA, or the U.S. Government. The U.S. Government is authorized to reproduce and distribute reprints for Governmental purposes notwithstanding any copyright annotation thereon.

## References

- [1] K. Bousmalis, G. Trigeorgis, N. Silberman, D. Krishnan, and D. Erhan. Domain separation networks. In *Advances in Neural Information Processing Systems 29: Annual Conference on Neural Information Processing Systems 2016*, 2016. 3
- [2] H. Daume III. Frustratingly easy domain adaptation. In *Proceedings of the 45th Annual Meeting of the Association of Computational Linguistics*, June 2007. 2
- [3] Y. Ganin and V. Lempitsky. Unsupervised domain adaptation by backpropagation. *arXiv preprint arXiv:1409.7495*, 2014. 2, 5, 6, 7, 8
- [4] M. Ghifary, W. B. Kleijn, M. Zhang, D. Balduzzi, and W. Li. Deep reconstruction-classification networks for unsupervised domain adaptation. In *European Conference on Computer Vision*. Springer, 2016. 2, 3, 5, 7, 8
- [5] X. Glorot and Y. Bengio. Understanding the difficulty of training deep feedforward neural networks. In *Aistats*, volume 9, 2010. 7, 8
- [6] B. Gong, Y. Shi, F. Sha, and K. Grauman. Geodesic flow kernel for unsupervised domain adaptation. In *2012 IEEE Conference on Computer Vision and Pattern Recognition*, pages 2066–2073, 2012. 2, 8
- [7] I. Goodfellow, J. Pouget-Abadie, M. Mirza, B. Xu, D. Warde-Farley, S. Ozair, A. Courville, and Y. Bengio. Generative adversarial nets. In *NIPS*, 2014. 2
- [8] R. Gopalan, R. Li, and R. Chellappa. Domain adaptation for object recognition: An unsupervised approach. In *Proceedings of the 2011 International Conference on Computer Vision, ICCV '11*, 2011. 2
- [9] K. He, X. Zhang, S. Ren, and J. Sun. Deep residual learning for image recognition. In *Proceedings of the IEEE Conference on Computer Vision and Pattern Recognition*, 2016. 1, 2
- [10] J. Huang, A. J. Smola, A. Gretton, K. M. Borgwardt, and B. Scholkopf. Correcting sample selection bias by unlabeled data. In *Proceedings of the 19th International Conference on Neural Information Processing Systems, NIPS'06*, 2006. 2
- [11] J. J. Hull. A database for handwritten text recognition research. *IEEE Transactions on pattern analysis and machine intelligence*, 16(5):550–554, 1994. 5
- [12] D. P. Kingma and J. Ba. Adam: A method for stochastic optimization. *CoRR*, abs/1412.6980, 2014. 6
- [13] A. Krizhevsky, I. Sutskever, and G. E. Hinton. Imagenet classification with deep convolutional neural networks. In *Advances in neural information processing systems*, 2012. 1, 2, 7
- [14] Y. LeCun, L. Bottou, Y. Bengio, and P. Haffner. Gradient-based learning applied to document recognition. *Proceedings of the IEEE*, 86(11), 1998. 5
- [15] M.-Y. Liu and O. Tuzel. Coupled generative adversarial networks. In D. D. Lee, M. Sugiyama, U. V. Luxburg, I. Guyon, and R. Garnett, editors, *Advances in Neural Information Processing Systems 29*, pages 469–477. 2016. 3, 5
- [16] M. Long, Y. Cao, J. Wang, and M. I. Jordan. Learning transferable features with deep adaptation networks. In *Proceedings of the 32nd International Conference on Machine Learning*, pages 97–105, 2015. 2, 8
- [17] M. Long, J. Wang, G. Ding, J. Sun, and P. S. Yu. Transfer feature learning with joint distribution adaptation. In *IEEE International Conference on Computer Vision, ICCV 2013*. IEEE Computer Society, 2013. 6
- [18] M. Long, J. Wang, and M. I. Jordan. Unsupervised domain adaptation with residual transfer networks. *CoRR*, abs/1602.04433, 2016. 2, 7, 8
- [19] L. v. d. Maaten and G. Hinton. Visualizing data using t-sne. *Journal of Machine Learning Research*, 9, 2008. 2
- [20] M. Mirza and S. Osindero. Conditional generative adversarial nets. *arXiv preprint arXiv:1411.1784*, 2014. 3
- [21] Y. Netzer, T. Wang, A. Coates, A. Bissacco, B. Wu, and A. Y. Ng. Reading digits in natural images with unsupervised feature learning. In *NIPS workshop on deep learning and unsupervised feature learning*, volume 2011, page 5, 2011. 5
- [22] S. J. Pan, I. W. Tsang, J. T. Kwok, and Q. Yang. Domain adaptation via transfer component analysis. In *Proceedings of the 21st International Joint Conference on Artificial Intelligence, IJCAI'09*, 2009. 2
- [23] A. Radford, L. Metz, and S. Chintala. Unsupervised representation learning with deep convolutional generative adversarial networks. *arXiv preprint arXiv:1511.06434*, 2015. 6
- [24] R. Ranjan, V. M. Patel, and R. Chellappa. Hyperface: A deep multi-task learning framework for face detection, landmark localization, pose estimation, and gender recognition. *arXiv preprint arXiv:1603.01249*, 2016. 8
- [25] S. Sankaranarayanan, A. Alavi, C. D. Castillo, and R. Chellappa. Triplet probabilistic embedding for face verification and clustering. In *Biometrics Theory, Applications and Systems (BTAS), 2016 IEEE 8th International Conference on*, pages 1–8. IEEE, 2016. 8
- [26] F. Schroff, D. Kalenichenko, and J. Philbin. Facenet: A unified embedding for face recognition and clustering. In *Proceedings of the IEEE Conference on Computer Vision and Pattern Recognition*, 2015. 1
- [27] S. Sengupta, J. C. Chen, C. Castillo, V. M. Patel, R. Chellappa, and D. W. Jacobs. Frontal to profile face verification in the wild. In *2016 IEEE Winter Conference on Applications of Computer Vision (WACV)*, pages 1–9, March 2016. 7

- [28] A. Sharif Razavian, H. Azizpour, J. Sullivan, and S. Carlsson. Cnn features off-the-shelf: an astounding baseline for recognition. In *Proceedings of the IEEE Conference on Computer Vision and Pattern Recognition Workshops*, 2014. [1](#)
- [29] Y. Taigman, A. Polyak, and L. Wolf. Unsupervised cross-domain image generation. *CoRR*, abs/1611.02200, 2016. [2](#), [3](#)
- [30] E. Tzeng, J. Hoffman, K. Saenko, and T. Darrell. Adversarial discriminative domain adaptation. *CoRR*, abs/1702.05464, 2017. [2](#), [5](#), [6](#)
- [31] E. Tzeng, J. Hoffman, N. Zhang, K. Saenko, and T. Darrell. Deep domain confusion: Maximizing for domain invariance. *CoRR*, abs/1412.3474, 2014. [2](#), [7](#), [8](#)
- [32] J. Yosinski, J. Clune, Y. Bengio, and H. Lipson. How transferable are features in deep neural networks? In *Advances in Neural Information Processing Systems 27: Annual Conference on Neural Information Processing Systems 2014*, 2014. [7](#)